Proceedings of the Pakistan Academy of Sciences 48 (1): 19–32, 2011

ISSN: 0377 - 2969


Pakistan Academy of Sciences

Satellite-Based Snowcover Distribution and Associated Snowmelt Runoff Modeling in Swat River Basin of Pakistan

Zakir H. Dahri[1*], Bashir Ahmad[1], Joseph H. Leach[2] and Shakil Ahmad[3]

[1] Pakistan Agricultural Research Council, Islamabad, Pakistan
[2] Department of Geomantic, The University of Melbourne, Australia
[3] National University of Science and Technology, Islamabad, Pakistan

Abstract: The snowcover and glaciers of Hindu Kush–Himalayan (HKH) region are one of the largest repositories of inland cryosphere outside Polar Regions and obviously the lifeline for the people of sub-continent. However, reliable estimates of the snow area extent and snowmelt runoff have been lacking in this largely inaccessible and data sparse region. This is particularly important in view of the climate change impacts on hydrological resources of the region. Present study utilized GIS, RS and hydrological modeling techniques to estimate spatial and temporal distribution of snowcover; quantified snowmelt and rainfall runoff components; and developed prediction models for snowmelt and river discharges. The results revealed that Swat River Basin of Pakistan is predominantly snow-fed, as the annual snowmelt runoff contribution to the total runoff may range 65–75 %. A significant effect of snowcover variation was observed on river discharge and snowmelt runoff. Snowcover and associated snowmelt runoff remain highly variable throughout the calendar year. Snowfall usually starts abruptly in September and October months but the following four main winter months (i.e., November–February) generally bring in most of the snowfall. Snowcover increases from less than 2 % of the Basin area in August, only at higher altitudes, to about 64 % by the end of January or early February. Snowmelt generally continues throughout the year but contribution of winter snowmelt runoff is generally very low. Unlike snowfall, snowmelt runoff usually progresses gradually and smoothly and is more predictable. The summer snowmelt normally gets momentum in March and increases from around 30–60 m^3/sec to 400-760 m^3/sec in late June or early July. Thereafter, it declines gradually, reducing to 30-50 m^3/sec in December. The December–February runoff normally remains the same.

Keywords: Snowcover, snowmelt, runoff, hydrological modeling, GIS, RS

INTRODUCTION

Snow and glaciers are the frozen reservoirs of fresh water and cover a significant part of many mountain chains on the globe. In Pakistan about 5218 glaciers covering an area of 15,040 sq km were identified in the ten sub-basins of Indus River System [1]. These glaciers constitute 11.7 % of the total area of these basins and are an important source of fresh water in Pakistan as 50 – 85 % of the country's total flows come from melting snows and glaciers of the this region [1, 2, 3]. The major tributaries of the Indus River originate from the Hindu Kush-Himalayan (HKH) region and have their upper catchments in the high mountain snow covered areas and flow through steep mountainous slopes. The planning of new projects on HKH rivers in Pakistan emphasizes the need for reliable estimates of the snow extent and glacier runoff because it provides a more dependable and perennial flow. Despite their well recognized importance and potential, little attempts have been made to assess in detail the contributions of snowmelt runoff in these rivers.

No detailed investigation of snow and ice processes or their relevance to climate has taken place in most areas of the Himalayan and other high ranges. Baseline studies are lacking for most areas, particularly for those higher than 4,000 masl, and there has been little long-term

Received June 2010, Accepted March 2011
*Corresponding author: Zakir H. Dahri; E-mail: zakirdahri@yahoo.com

monitoring of climatic variables, perennial snow and ice, runoff and hydrology in the extremely heterogeneity of mountain topography [4]. In the areas where bulk of the water originates, above 3000 meters or so, there are no permanent observation stations. The main need is for the investigation of water resources at elevations between 3000 to 7000 meters. There is a dire need for cryosphere database development and to study the impact of climate change on the cryosphere. Remote sensing techniques are the only way to analyze glaciers in remote mountains and they are certainly the only way to monitor a large number of glaciers simultaneously.

Recent advances in GIS, remote sensing and hydrological modeling techniques allow their powerful integration. In the field of snowmelt runoff modeling, such integration provides valuable basis for better understanding of snow accumulation and snowmelt runoff processes within the catchments, as well as for incorporating the spatial variability of hydrological and geographical variables and their impacts on catchment responses [5].

Rango et al. [6] employed snow-covered area data obtained from meteorological satellites over remote regions of Pakistan and concluded that it can be scientifically related to seasonal stream flow in regression analysis for the Indus River above Besham and Kabul River above Nowshera in Pakistan [6]. Combining the remote sensing derived snow and ice cover maps with a hydrologic runoff model the daily runoff can be calculated [7, 8]. Snow and icemelt are important contributors to the total yearly runoff volume in high alpine basins. Schaper and Seidel [9] carried out runoff simulations for snow and icemelt for the basins of Rhine-Felsberg, Rhône-Sion and Ticino-Bellinzona. This study provides a method to calculate runoff from snow- and icemelt using meteorological data and remote sensing derived snow and ice cover maps.

The Snowmelt Runoff Model (SRM) is one of a very few models in the world today that requires remote sensing derived snow cover as model input. Owing to its simple data requirements and use of remote sensing to provide snow cover information, SRM is ideal for use in data sparse regions, particularly in remote and inaccessible high mountain watersheds [10].

Runoff computations by SRM appear to be relatively easily understood. To date the model has been applied by various agencies, institutes and universities in over 100 basins, situated in 29 different countries. More than 80% of these applications have been performed by independent users, as is evident from 80 references to pertinent publications. SRM also successfully underwent tests by the World Meteorological Organization with regard to runoff simulations [11] and to partially simulated conditions of real time runoff forecasts [12].

Seidel et al. [13] successfully simulated the runoff in the large Himalayan Basin, e.g. Ganges and Brahmaputra basins, by applying SRM [13]. SRM performs well in the Gongnaisi River basin and results also show that SRM can be a suitable snowmelt runoff model capable of being applied in the western Tianshan Mountains [10]. Emre et al. [14] applied SRM in upper Euphrates River using MODIS-8 daily snow cover products for 2002-04. The initial results of their modeling process show that MODIS snow-covered area product can be used for simulation and also for forecasting of snowmelt runoff in basins of Turkey. The SRM application in Kuban river basin using MOD10A2 eight-day composite snow cover data enabled the investigator to conclude that the model can be used for short-term runoff forecasts in the mountain and foothill areas of the Krasnodar reservoir basin [15].

Climate change is likely to affect basin's water resources so there is a need to monitor and estimate the fresh water resource base (snowcover) and assess the impacts of its variation on net water availability. Present study has been conducted in Swat River Basin which is snowfed and source of fresh water especially in summer season. The specific objectives of this research study are:

- Estimation of spatial and temporal distribution of snowcover through satellite remote sensing;
- Estimation and quantification of snowmelt and rainfall runoff components through hydrological modeling; and
- Development of snowmelt runoff prediction models.

Characteristics of the Study Area

The study was undertaken in the catchment area of Swat River upstream of Chakdara gauge. The study area is located between the latitude and longitude range of 34.57 to 35.9 and 71.9 to 72.8 decimal degrees respectively covering an area of 5713.4 km^2. Its northern part has high mountainous of rugged terrain with elevation range of 2000–5808 m a.s.l., whereas the southern part is relatively flat with elevation range of 686–2000 m a.s.l. having some crop fields on either side of the river as shown in Fig. 1.

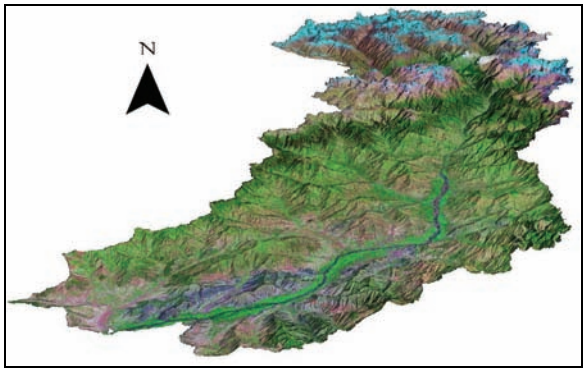

Fig. 1. True color LANDSAT image of the study area .

Based on the historic as well as prevailing climatic conditions, the study area can be divided into two parts. The upper north-eastern part – Kalam and surrounding areas – comprises very rugged mountain topography and may reach a maximum temperature of 37 °C in June at Kalam to as low as –18.2 °C in January at Shandur. The lower south-eastern part near Saidu Sharif and Chakdara is relatively flat, having considerably higher temperatures ranging from -2 °C in January to as high as 45 °C in June. Similarly, the precipitation pattern in the lower south-western part is influenced by the summer monsoon rainfall. The upper north-eastern part on the other hand is dominated by the winter rainfall mainly received from the Western Disturbances, which come from the Mediterranean Sea after passing through Iran and Afghanistan enter Pakistan in December and continue till early April. The northern highlands receive most of winter precipitation in the form of snow 1 km at nadir. The 1st two bands were imaged at a nominal resolution of 250 m at nadir, next five bands at 500 m, and the remaining 29 bands at 1 km. The MODIS snow products use only the 1st seven and last two bands between 0.405 and 14.385 µm for different uses. Its spatial resolution varies with spectral band, and ranges from 250 m to instrument acquires images in 36 spectral.

METHODOLOGY

The methodology employed to accomplish this study is summarized in the flow chart shown in Fig. 2. The important steps are described in the following paragraphs.

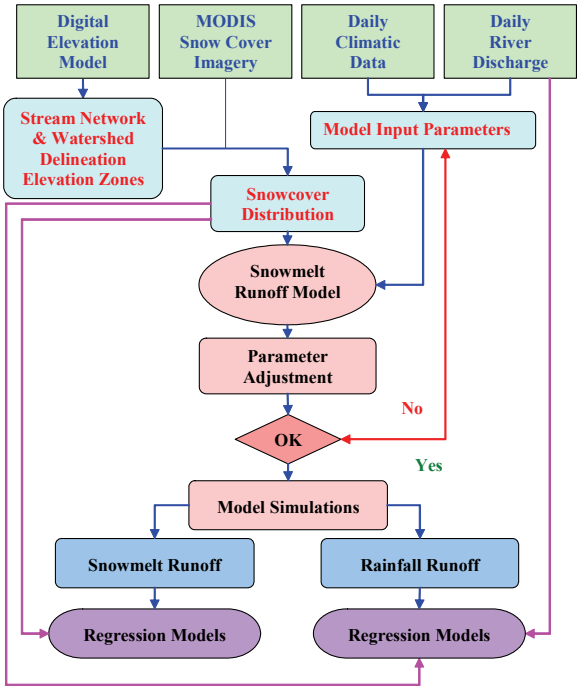

Fig. 2. Flow diagram of the methodological approach.

Snowcover Estimation

The snowcover was estimated using the Snowcover products of MODIS (Moderate Resolution Imaging Spectroradiometer) instrument onboard the Terra spacecraft launched on December 18, 1999 and the Aqua spacecraft, launched on May 4, 2002. Terra's orbit around the Earth is timed so that it passes from north to south across the equator in the morning, while Aqua passes south to north over the equator in the afternoon.

The development of the MODIS snow mapping algorithm (snowmap) is chronicled in detail by [16–21]. The basic techniques used in

the snowmap algorithm are grouped-criteria incorporating the normalized difference between bands, threshold-based criteria tests, and decision rules [18]. The first test of snow detection uses the Normalized Difference Snow Index (NDSI) approach, which is an effective way to distinguish snow from many other Generally, snow is characterized by higher NDSI values than other surface types and pixels. A pixel is mapped as snow if the NDSI value is ≥ 0.4 and the reflectance in MODIS band 2 is greater than 0.11. However, if the reflectance in MODIS band 4 is less than 0.10 then the pixel will not be mapped as snow even if the other criteria are met [18, 19]. This minimum reflectance test screens low reflectance surfaces, e.g. water that may have a high NDSI value from being erroneously detected as snow. However, in forest areas snow-covered pixels may have considerably lower NDSI values and to correctly classify these pixels as snow covered, NDSI and NDVI are used together to the pixels that have an NDSI value in the range of 0.1 to 0.4. The NDVI is calculated as:

$$NDVI = \frac{Band2 - Band1}{Band2 + Band1}$$

Snow cover tends to lower the NDVI therefore pixels with NDVI value of ≈ 0.1 may be mapped as snow even if the NDSI < 0.4 [17]. Moreover, pixels with an absolute reflectance greater than 0.11 in MODIS band 2 & greater than 0.10 in MODIS band 1 are labeled as snow.

Because of higher reflectance of clouds in near-infrared wavelengths the NDSI generally separates snow from most obscuring cumulus clouds, but it cannot always discriminate optically-thin cirrus clouds from snow. Instead, cloud discrimination is accomplished by using the MODIS cloud mask product, MOD35L2, [22, 23], which employs a series of visible and infrared threshold and consistency tests to specify confidence that an unobstructed view of the Earth's surface is observed. An indication of shadows affecting the scene is also provided.

Land and inland waters are masked with the 1 km resolution land/water mask, contained in the MODIS geolocation product (MOD03). Thermal mask is used to improve the snow mapping accuracy and to eliminate the spurious snow especially in warm climates. Using MODIS infrared bands 31 (10.78–11.28 μm) and 32 (11.77–12.27 μm), a split window technique [24] is used to estimate ground temperature [19]. surface features taking advantage of strong visible reflectance and strong short-wave IR absorbing characteristics of the snow pack. The NDSI is defined as:

$$NDSI = \frac{Band4 - Band6}{Band4 + Band6}$$

If the temperature of a pixel is greater than 283 ^{0}K then the pixel will not be mapped as snow [21].

Fractional snow cover is calculated using the regression equation of Salomonson and Appel [25], which is based on a statistical-linear relationship developed between the NDSI from MODIS and the true sub-pixel fraction of snow cover as determined using Landsat scenes from Alaska, Canada and Russia. The data inputs to the MODIS snowmap algorithm are summarized in Table 1.

Table 1. MODIS data product inputs to the MODIS snowmap algorithm.

Earth Science Data Type (ESDT)	Long Name	Data Used
MOD02HKM	MODIS Level 1B Calibrated Geolocated Radiances	Reflectance for MODIS bands: 1 (0.645 μm) 2 (0.865 μm) 4 (0.555 μm) 6 (1.640 μm)
MOD021KM	MODIS Level 1B Calibrated & Geolocated Radiances	31 (11.28 μm) 32 (12.27 μm)
MOD03	MODIS Geolocation	Land/Water Mask Solar Zenith Angles Sensor Zenith Angles Latitude Longitude
MOD35L2	MODIS Cloud Mask	Cloud Mask Flag Unobstructed Field of View Flag Day/Night Flag

Source: After [21]

The accuracy of snowmap has been tested over a variety of surface covers relative to other derived snow cover maps. Under ideal conditions of illumination, clear skies and several centimeters of snow on a smooth surface

the snow algorithm is about 93-100% accurate at mapping snow [20]. Lower accuracy is found in forested areas and complex terrain and when snow is thin and ephemeral. Very high accuracy, over 99%, may be found in croplands and agricultural areas.

Snow Melt Runoff Model

The snowmelt runoff model (SRM), also known as "Martinec-Rungo Model" [26] is a semi-distributed, deterministic and degree-day hydrological model especially designed to simulate and forecast daily stream flow inmountain basins where snowmelt is major runoff factor [27]. The model utilizes ambient air temperature values combined with a degree-day coefficient in order to estimate the ablation factor of the snow cover and takes input of snow covered area and its variation along meteorological data. The basin area is divided in to a suitable number of elevation zones (not exceeding 16) and various input parameters including basin characteristics, climatic variables, snow covered area, runoff co-efficients, recession coefficients, etc are specified for each elevation zone. The model manages a physical database of both input and output for a given basin. Each simulation in the model is a unique entity operating on a 2– 366 days. Different simulations can be sequenced for greater time periods. The SRM computes daily water produced from snowmelt and rainfall, superimposes it on the calculated recession flow and transforms it into daily discharge from the basin according to the following equation.

$$Q_{n+1} = \left[c_{Sn} a_n (T_n + \Delta T_n) S_n + c_{Rn} P_n\right] \frac{A.10000}{86400} (1 - k_{n+1}) + Q_n k_{n+1}$$

Where:

Q = average daily discharge [$m^3 s^{-1}$]

c = runoff coefficient expressing the losses as a ratio (runoff/precipitation), with c_S referring to snowmelt and c_R to rain

a = degree-day factor [cm $^oC^{-1}$ d^{-1}] indicating the snowmelt depth resulting from 1 degree-day

T = number of degree-days [^oC d]

ΔT = the temperature lapse rate correction factor [^oC d]

S = ratio of the snow covered area to the total area

P = precipitation contributing to runoff [cm]. A pre-selected threshold temperature, T_{CRIT}, determines whether this contribution is rainfall (immediate) or snow (delayed).

A = area of the basin or zone [km^2]

k = recession coefficient indicating the decline of discharge in a period without snowmelt or rainfall. K = Q_{m+1}/Q_m (m, m + 1 are the sequence of days during a true recession flow period).

n = sequence of days during the discharge computation period. Equation (1) is written for a time lag between the daily temperature cycle and the resulting discharge cycle of 18 hours. In this case, the number of degree-days measured on the n^{th} day corresponds to the discharge on the n + 1 day. Various lag times can be introduced by a subroutine.

10000/86400 = conversion from cm·km^2 d^{-1} to m^3 s^{-1}

Derivation of Model Input Parameters

The input data requirements of the SRM are categorized into three categories i.e. basin characteristics, variables and parameters. The basin characteristics are usually computed from the digital elevation model of the area. The variables include temperature, precipitation and snowcover. The actual/observed records of temperature and precipitation are available while snowcover is estimated from MODIS satellite imagery. The parameters are temperature lapse rate, critical temperature, degree day factor, time lag, runoff coefficient, rainfall contributing area, and recession coefficient. These parameters can be computed from field measurements, derived from the variables or determined through physical laws. In cases where actual data are not available, adjustment and refinement of certain parameters within permissible limits during model verification is usually done.

Basin Characteristics

The watershed and river network has been delineated from the SRTM DEM data of the Swat basin using ArcHydro extension of ArcGIS software. Since, the SRM represents a semi-distributed approach, considering each catchment section with similar hydrological characteristics as a single unit (hydrological response unit, HRU), the basin has been divided

into five elevation zones (Zone-A to Zone-E) keeping in view the available elevation range of 686 m–5808 m as shown in Fig. 3. The total area of the basin is 5713.38 sq. km with a mean hypsometric elevation of 2727.2 m. The mean hypsometric elevations for each elevation zone are 1133.42, 1956.63, 3014.76, 4007.57, 4726.55 m respectively.

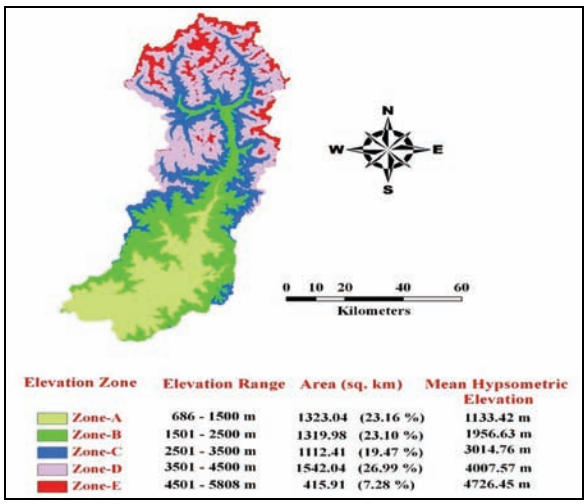

Fig. 3. Elevation zones, their areas & mean hypsometric elevation.

Variables

The daily meteorological data for a number of met stations in the vicinity of study basin has been acquired from Pakistan Meteorological Department (PMD) and Surface Water Hydrology Project of WAPDA. The study utilizes temperature data of Kalam observatory for each elevation zone. For precipitation, data of Saidu Sharif (961 m amsl) is used for Zone A, Kalam (2103 m amsl) for Zones B, C, and D and Shandur (3719 m amsl) for Zone E. Snowcover extent in the watershed and in each elevation zone has been determined from the eight daily MOD10A2 MODIS snowcover product. A total of 138 satellite images spread over a period of three years (1st January 2002 to 31st December 2004) are processed through ERDAS Imagine and ArcGIS softwares.

Temperature lapse rate: The temperature lapse rate due to elevation difference is estimated by plotting the temperature records of a number of met stations located in the vicinity of study basin. The computed temperature lapse rates for January to December months are 0.68, 0.69, 0.69, 0.67, 0.70, 0.73, 0.62, 0.61, 0.64, 0.68, 0.66, and 0.65 ^{0}C / 100 m respectively.

Degree day factor: Since, the average temperatures always refer to a 24 hour period starting at 6.00 hrs; they become degree-days, T (^{0}C.d). The degree-day factor (a) can be determined by comparing degree-day values (temperature values above a certain base temperature) with the daily decrease of snow water equivalent (SWE). However, the data on variation of SWE is rarely available. In the absence of any detailed data, the degree day factor can be calculated from the following empirical relation [27]:

$$a = 1.1.\frac{\rho_s}{\rho_w}$$

Where: a is the degree day factor (cm/^{0}C/d), and ρ_s & ρ_w are densities of snow and water respectively. Density of snow usually varies from 0.3 to 0.55 gm/cc resulting in value of degree-day factor in the range of 0.35 – 0.61, with lower value recommended for fresh snow and snow under forest canopy. However, slightly higher values have also been reported in the snow melt runoff modeling studies [27]. The degree-day factor converts the number of degree-days T [^{0}C·d] into the daily snowmelt depth M [cm] by the following relation:

$$M = a.T$$

Critical temperature: Critical temperature determines whether the precipitation is in the form of rain or snowfall. Usual values ranging from +3^{0}C in April to 0.75^{0}C in July are reported [26] with higher values in snow accumulation periods. A similar trend with a narrower range +1.5^{0}C to 0^{0}C is reported by US Army Corps of Engineers [29]. It is very difficult to differentiate exactly between rain and snow because the temperature used is the daily average while precipitation may occur at any time during the day and that particular moment may be warmer or colder than the assigned temperature value. SRM needs the critical temperature only in the snowmelt season in order to decide whether precipitation immediately contributes to runoff, or, if T < TCRIT, whether snowfall took place. This parameter is more important for year round simulations which model both snow accumulation and snow ablation periods.

Rainfall contributing area: Snow pack is usually dry before and during early snowmelt season and most of the rain falling on snow pack is normally retained by it. Only snow free area contributes to rainfall runoff during that period. However, at

some later stage the snow pack becomes wet and the rain falling afterwards can flow as runoff. The user has to decide which time periods snow pack in a particular area and height will be dry and assign that input to the model accordingly. The melting effect of rain however is neglected because the additional heat supplied by the liquid precipitation is considered to be very small [30].

Runoff coefficient: The runoff coefficient takes care of the losses from the basin's available water resources (rain + snow) during its conveyance to the outlet. The average value of runoff coefficient for a particular basin is given by the ratio of annual runoff to annual precipitation. The comparison of historical precipitation and runoff ratios provide starting point for estimation of runoff coefficient. However, more often it varies throughout the year as a result of changing temperature, vegetation and soil moisture conditions. Moreover, very high uncertainty involved in the measurement of true representative precipitation poses serious difficulties in its correct estimation. For this reason, among SRM parameters, the runoff coefficient is the primary candidate for adjustment during model calibration [27]. Runoff coefficient is usually higher for snow melt than for rainfall due to effect of cold water soil hydraulic conductivity.

Recession coefficient: Stream flow recession represents withdrawal of water from the storage with no or little inflow. River discharge data of Chakdara gauge station, which is located at the exit point of the basin, was collected from Surface Water Hydrology Project (SWHP) of Water and Power Development Authority (WAPDA), Pakistan. The discharge on a given day (Q_n) is plotted on the logarithmic scale against the value of discharge on the following day (Q_{n+1}) as shown in the Fig. 4. An envelop is drawn to enclose most of the points and the lower envelop line of all points is considered to indicate the k-values.

For $Q_{n+1} = 700$ and $Q_n = 900$, the value of k is derived from relation $k = Q_{n+1} / Q_n$, or $k = 700/900 = 0.777$. Similarly, the value of k_2 can be derived from the other corresponding values of Q_{n+1} and Q_n. It is observed that the value of k increases with decreasing Q, by solving the equation $k_{n+1} = x.Q_n^{-y}$, the values of constants x and y are computed for two corresponding Q and k values.

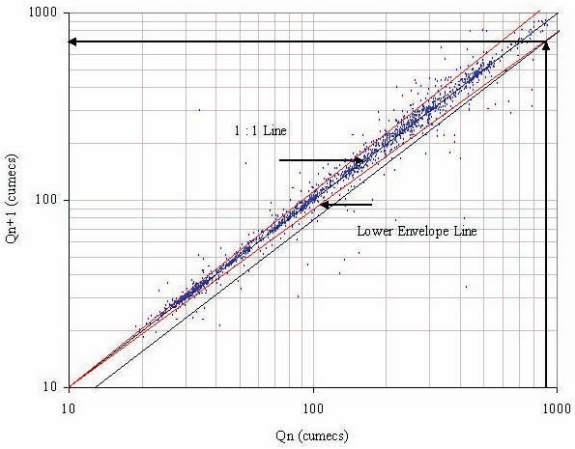

Fig. 4. Recession flow plot Q_n vs Q_{n+1} for the Swat River Basin of Pakistan.

Time lag: For large basins with multiple elevation zones, the time lag changes during the snowmelt season as a result of changing spatial distribution of snow cover with respect to the basin outlet. Generally the time lag in a basin increases as the snow line retreats. If there is uncertainty, the time lag can be adjusted in order to improve the synchronization of the measured and simulated peaks of average daily flows.

Model Calibration and Verification

The mountain hydrology is mainly the function of topography and meteorology however the knowledge about interaction of these components of mountain hydrology is generally limited and qualitative in nature [31]. Therefore, there is more reliance on river flow data of the mountain areas which largely represent the hydrological responses of all the existing topographical factors and meteorological events taking place in the mountain regions [32, 33].

The SRM normally does not require calibration as its input parameters are generally derived from the field data and historical records through physical laws and empirical relationships. However, gathering of all the required data is only a dream for a highly rugged mountain terrain in a country like Pakistan, where inaccessibility and lack of resources generally limit collection of such data. Hence, calibration of the model and some rational adjustment of few input parameters are unavoidable and in fact the user gains more confident over the simulation results. Therefore, some of the parameters were adjusted during calibration and verification against the daily

river inflows of year 2002 to 2004. Besides visual inspection, the accuracy of calibration was judged from the two well established accuracy criteria [27], the coefficient of determination (R^2) and the deviation of runoff volumes (Dv).

RESULTS AND DISCUSSION

Spatial and Temporal Distribution of Snowcover

Determining contribution of snowmelt runoff to river discharges has great practical significance as snowmelt runoff is more dependable source of fresh water. Unfortunately, the highly rugged ground control to accurately monitor metrological data and snowcover information on a continuous basis. In such circumstances satellite remote sensing has great value and seems to be the only viable alternative, as it can provide repetitive data on snow area extent at different, regular time intervals. The study utilized MODIS snowcover products to estimate snow area extent in the Swat River Basin of Pakistan. The MODIS 8-daily (level 3, version 5) maximum snow extent composite snowcover product (MOD10A2) was processed in a RS and GIS environment to estimate spatial and temporal variation of snow cover in the basin. In all 140 images distributed over three years period (Jan. 2002 to Dec. 2004), were processed and analyzed. Fig. 5 presents temporal (on daily basis) variation of snowcover at various elevation zones for the three years period, while Fig. 6 shows spatial distribution of snowcover through the sequence of selected time series GIS processed snowcover maps of the basin for the same period.

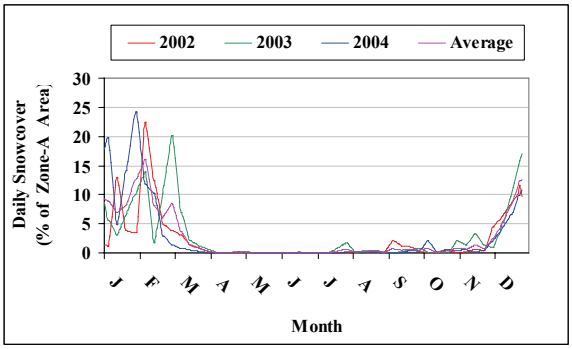

a. Snowcover distribution in Zone-A

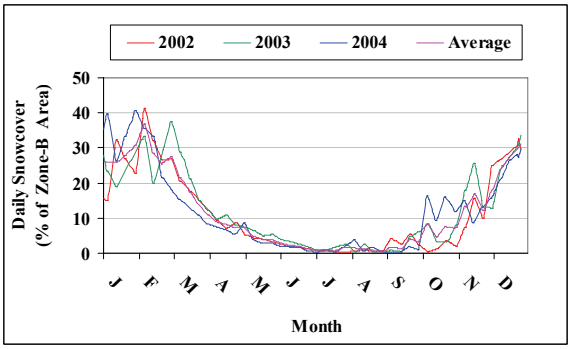

b. Snowcover distribution in Zone-B

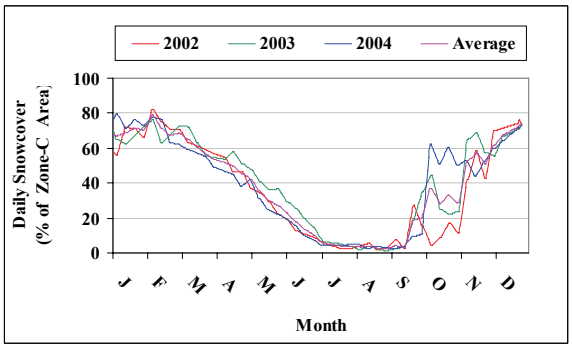

c. Snowcover distribution in Zone-C

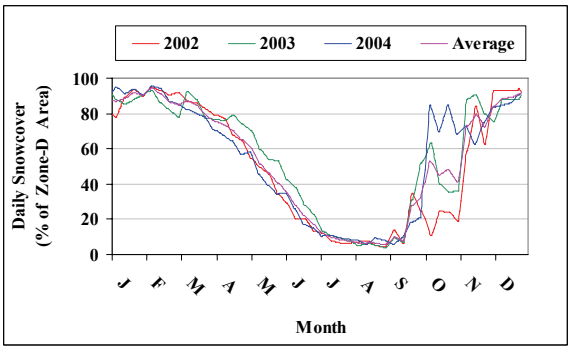

d. Snowcover distribution in Zone-D

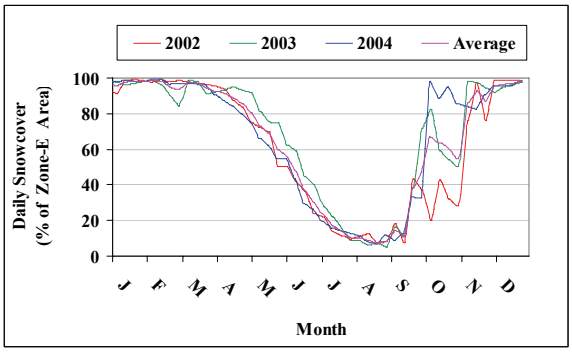

e. Snowcover distribution in Zone-E

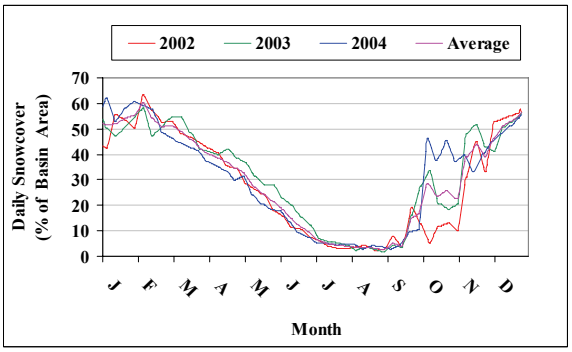

f. Snowcover distribution in Zone-F

Fig. 5. Temporal variation of snowcover at various elevation zones for the three years period.

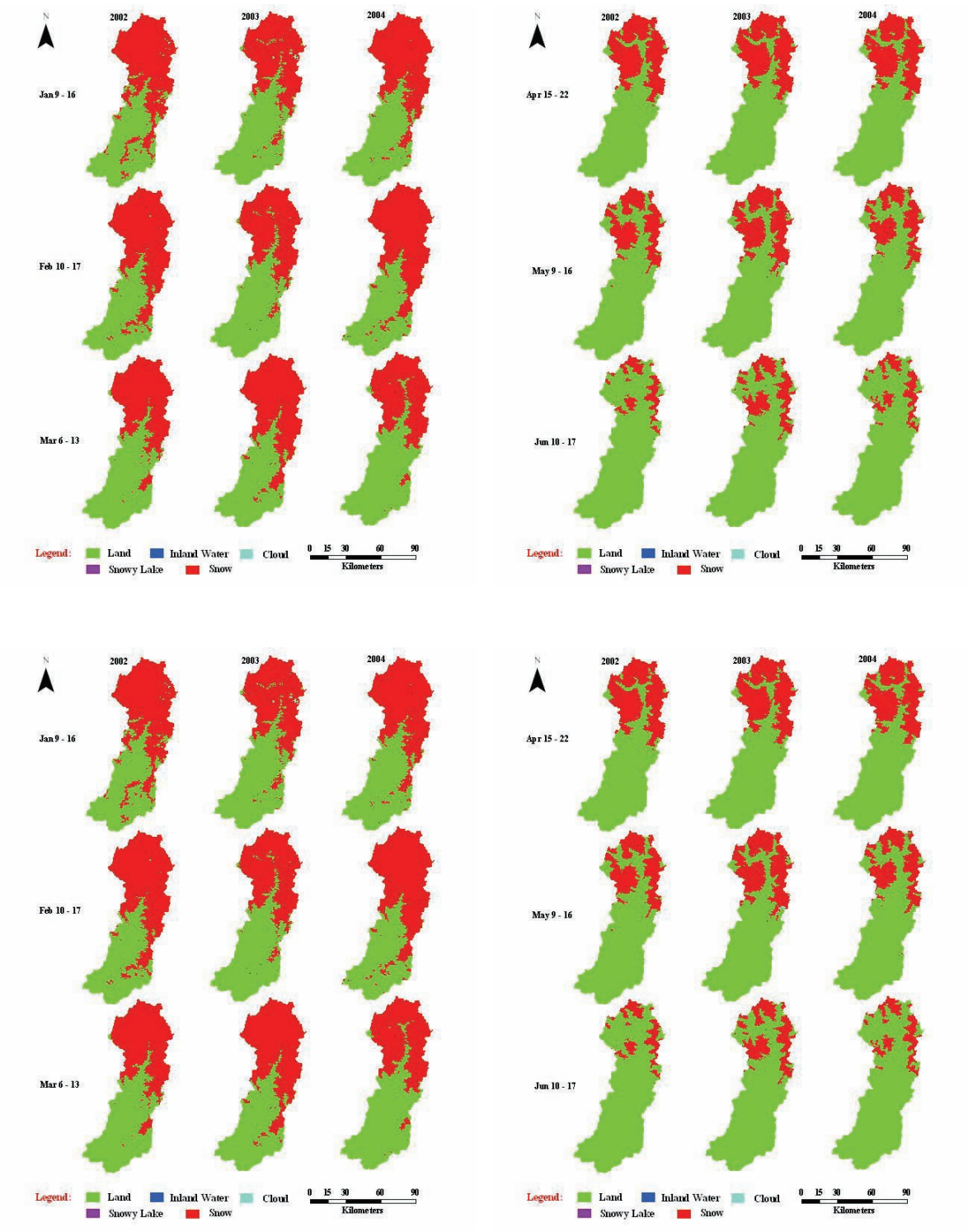

Fig. 6. Snowcover variation during Jan – Mar, Apr – Jun, Jul – Aug, and Sep – Dec.

The analysis and visual observation of the generated snowcover maps and developed graphs reveal that snowfall and subsequent snowmelt in the Swat river basin is highly variable in terms of altitude, space and time. The snowfall usually starts by the mid to late September initially at higher elevations and snow area may be increased abruptly from less than 2% in August to about 10–20 % of the total basin area. Occasional and unpredictable rainstorms in September and October months most often bring immediate, abrupt and significant increase in snowcover area and snowcover may cover about 45% of the total basin area by the end of October. However, the following few weeks are unable to maintain that

tempo due to temperature variation and consequently some decline in snowcover is usually observed in many cases due to subsequent and immediate melting of that fresh and temporary snowcover. The main winter months (Nov–Feb) generally bring in most of the snowfall and snowcover keeps accumulating reaching its peak area by the end of January or early February covering about 58 – 64 % of the basin area. Significant snowfall at lower elevations is also witnessed during these main winter months as the snowcover gets extended down to valleys in southern parts and snowline may reach at elevations less than 1500 m. At higher elevations above 3500 m a.s.l. snow may continue to fall even in March and April months (Fig. 5d, 5e) when snow area in 2003 increased during these months.

Snowmelt generally continues throughout the year but contribution of winter snowmelt runoff is often insignificant. Flow during the winter season is usually augmented from surface flow due to seasonal rains, sub-surface flow, and ground-water contribution and is termed as the base flow. Unlike snowfall, snowmelt usually progresses gradually and smoothly and is more easily predictable. The summer snowmelt normally gets momentum in the month of March which may also bring in some new snows at times of cold waves accompanied with precipitation particularly at higher elevations. The net outcome however is towards snowmelt. At first the snow starts disappearing rapidly from valleys at southern parts of the basin and from elevations less than 2500 m in early March, which gradually widens and the snowline retreats upward as the summer season progresses and temperature is increased. At elevations greater than 4500 snowmelt starts in late April and continues till mid September. During July to mid September temperatures are usually sufficient enough to melt the snow and snowmelt is mainly the function of available snow, which is mostly concentrated at highest elevations and is about to finish. Minimum snowcover is usually observed in the late August until the new snowfall season starts in September. During the monsoon season, the peak snowmelt runoff is augmented by monsoon rains to produce higher discharges and occasional peak floods sometimes destroy the infrastructure.

The three-year snowcover monitoring with remote sensing shows that under conducive climatic conditions, the maximum snow area extent may cover about 64 % of the total area of the basin during January-February to as low as 1.7 % in late August during the snowmelt season. However, spatial analysis of the three years snowcover maps as shown in Fig. 7 suggests that not always the same area receives snowfall. Table 2 further depicts that about 79.14 % of the area received snowfall at any time during 2002 – 2004. This area can be termed as area which generally accommodates temporary and seasonal snowfall. A handful of 20.72 % never received snowfall during that period; while only in 0.14 % (8.187 sq. km) of the basin area, snow cover remained in tact and could not be melted during that three years period. This area can be termed as permanent snow or glaciated area. It means that the entire basin predominantly accommodates temporary and seasonal snowcover, which is an important element of the hydrological cycle of the basin and major contributor to the basin's fresh water resources.

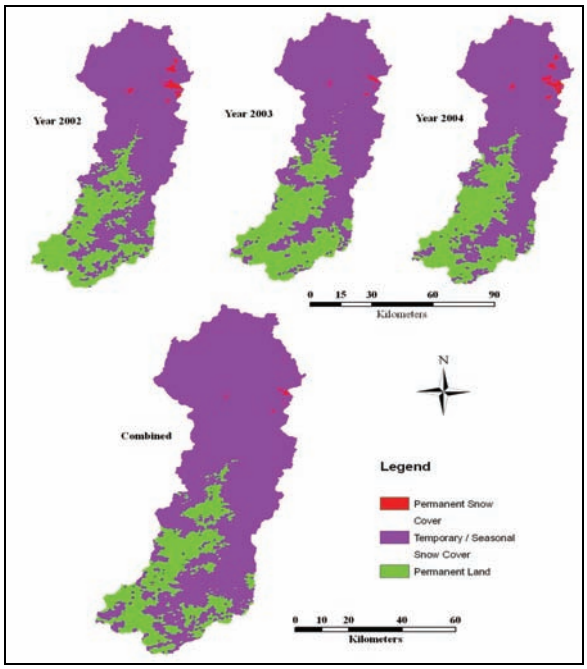

Fig. 7. Spatial analysis of permanent and temporary snow cover.

Table 2. Area under permanent and temporary snow covers for three study years.

Year	Permanent Land (sq km)	Temporary Snow (sq km)	Permanent Snow (sq km)
2002	1617.960 (28.32)	4043.269 (70.77)	52.150 (0.91)
2003	1809.644 (31.67)	3888.715 (68.06)	15.021 (0.26)
2004	1675.184 (29.32)	3981.328 (69.68)	56.867 (1.00)
2002–2004	1183.646 (20.72)	4521.546 (79.14)	8.187 (0.14)

Runoff Simulation Results

After estimation and derivation of all the model input parameters, the SRM was calibrated against the actually observed river flows during 2003. Some parameters were slightly adjusted and the calibrated model was verified for 2002 and 2004 river flows. Fig. 8 compares the simulated and actually observed river flows for years 2002, 2003 and 2004 while Table 3 assesses the accuracy of the simulation results by means of two statistical measures, i.e., coefficient of determination (R^2) and deviation of runoff volumes (D_v). The coefficient of determination is 0.796, 0.824 and 0.802 and the volume difference – 2.815%, - 4.077 %, and 3.202 % for 2002, 2003 and 2004 respectively. The calibration and verification results can be termed good and well within acceptable limits as SRM has been applied for over 112 basins in the past with 42% and -7.5 to +29.9% values of both these criteria, respectively [27]. Hence the calibrated and verified model can be used for simulation of any scenario.

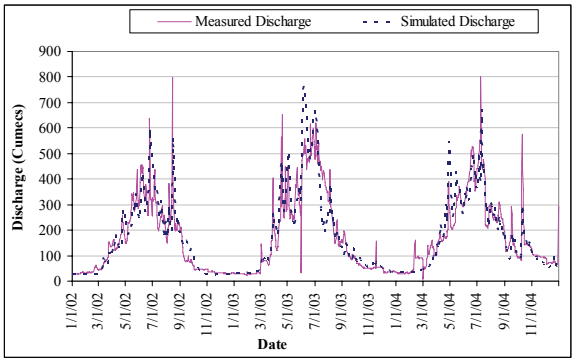

Fig. 8. Simulated and measured river flows.

Three scenarios have been developed in the present study. The first scenario runs the model with each year's own data and computes the daily runoff. The second scenario runs the model for each year's data but with no rainfall to calculate the respective share of snowmelt runoff into river discharge from the input of snowcover. The third scenario runs the model for each year with no rainfall and with normalized (putting historical average temperature values rather than each year's own temperature data) temperature. This scenario is developed to normalize the effect of temperature. It means whatever the effect of temperature is, it remains the same for each year and only the effect of snowcover change on snowmelt runoff is simulated.

Table 3. Year round simulation statistics for different study years.

Simulation Year	Measured Runoff Volume 10^6 m^3)	(Simulated Runoff Volume (10^6 m^3)	Volume Difference (%)	Coefficient of Determination (R^2)
2002	4465.18	4590.86	- 2.82	0.796
2003	5742.86	5977.02	- 4.08	0.824
2004	5874.32	5686.18	3.20	0.801

Simulated snowmelt and rainfall contribution components to runoff, computed through the SRM, are presented in Fig. 9. The figure clearly indicates the dominancy of snowmelt runoff as the basin is predominantly a snow-fed. However, there is also significant contribution of rainfall to runoff particularly in the summer monsoon moths of July and August. Snowmelt runoff contribution to the total runoff may ranges from 65–75 %. The results further suggest that about 30–60% of the total rain fall runoff occurs in monsoon season (July–September) and about 25–50 % in March to May period. The average contribution of snowmelt runoff to the total monthly runoff is 98.5, 91.2, 61.3, 61.6, 70.8, 83.0, 67.6, 53.3, 61.5, 73.1, 82.5, and 86.7 % for January–December months respectively.

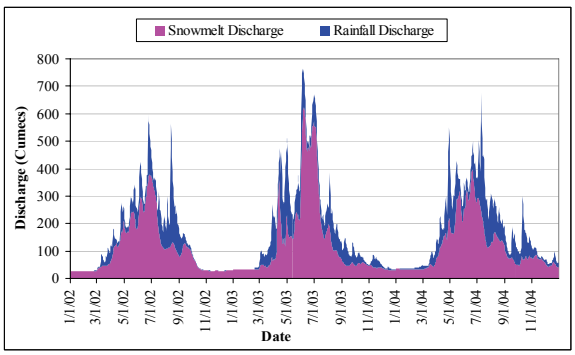

Fig. 9. Computed snowmelt and rainfall runoff components.

The study employed daily record of snowcover which show that snowfall can take place during eight months (September–April) and even minute amounts can be observed during the four main summer months. Therefore, relating winter snowcover with total summer runoff volume may give reasonable estimates for only the four main summer months (May–August). Instead this study not only relates the daily river discharges with the daily snow area extent but also develops prediction model for the total runoff volume of the four main summer months. The study also relates the simulated snowmelt runoff (excluding rainfall runoff component) with the snow area extent.

Fig. 10 clearly indicates a definite response of observed river discharges and simulated snowmelt runoff to seasonal snow cover changes, i.e. an increasing discharge associated with a decrease of snow area extent during the early summer (March-June), and decrease in discharge with decreasing snowcover in the late summer, monsoon season (July–August). Accordingly, two prediction models, described below, are developed to relate snowcover with river and snowmelt discharge.

Fig. 10(a) relates snow cover with river and snowmelt discharges for the early summer snowmelt season (March-June). This relationship can be described by the negative linear regression model as the river discharge increases with decrease in corresponding snowcover. Its relationship with the daily simulated snowmelt runoff is also negative but slightly different and is best explained by the third order polynomial function. This difference between the two regression models is due to variation of rainfall runoff component in the river discharges. Moreover, this inverse relationship is only true for the first part of the snowmelt season during which availability of snowcover is generally not a limiting factor and snowmelt runoff is largely the function of available temperature. But as the melting season progresses, the available snowcover gets depleted and it starts limiting the snowmelt runoff more than the temperature. Relationship between snowcover, snowmelt runoff and river discharge during the second part of the snowmelt season (July–August) as in Fig. 10(b) is completely different from that of the first part. During this summer monsoon period, most of seasonal snowcover at lower to medium elevations is melted and snowmelt runoff mainly comes from snowcover at high altitudes and permanent snow and glaciers of higher elevations. Unlike the previous model, this regression model shows positive relationship of average daily snowcover with the two runoffs. Also, there is exchange in type of regression model between the two relationships. The average daily snowcover now relates the simulated snowmelt runoff linearly, whereas its relationship with the average daily observed river discharge can be simplified by the second order polynomial function. The river discharge during the early July month tends to remain constant but greater river discharges in mid or late July than the early July month are due to greater contribution of rainfall runoff component during that period, otherwise snowmelt runoff decreases linearly during the following period.

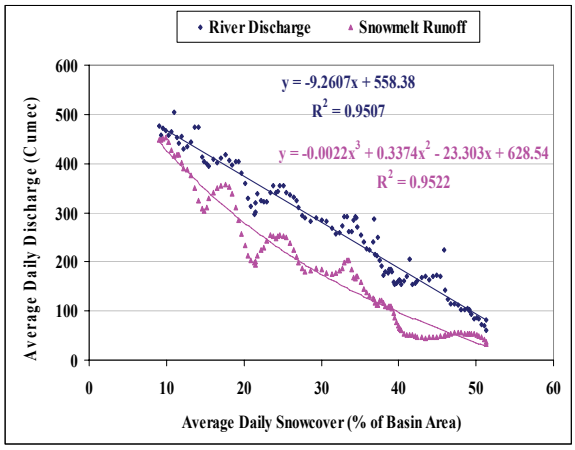

Fig. 10 (a) Relationship of daily snowcover with simulated snowmelt runoff and observed runoff for March–June months.

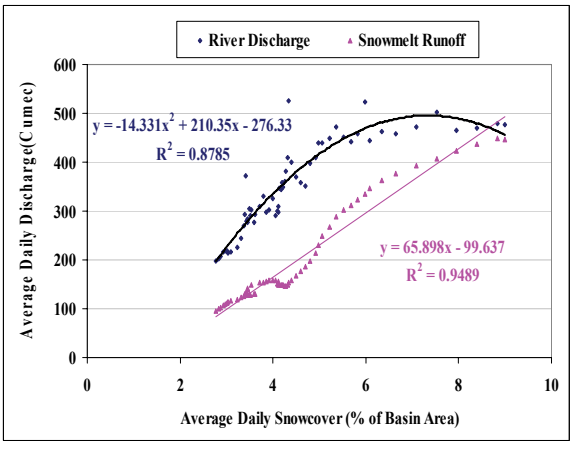

Fig. 10 (b) Relationship of daily snowcover with simulated snowmelt runoff and observed runoff for July–August months.

CONCLUSIONS

The altitudinal, spatial and temporal distribution of snowcover in the Swat River Basin of Pakistan was successfully evaluated using remotely sensed satellite imagery of the MODIS, GIS techniques and snowmelt runoff modeling. Increase in snowcover is observed in October and snow area extent sometimes may cover about 45 % of the basin area. The main winter months (i.e., November–February) generally bring in most of the snowfall and snowcover accumulates about 64 % from end of January or early February. The snowmelt normally starts in late February from lower elevation and increases gradually from around 30–60 m^3/sec to more than 400 m^3/sec to as high as 760 m^3/sec in late June or early July. The July–early September runoff is believed to be coming mainly from the melting of permanent snow and glacier melt at the highest elevations after most of the snowcover at lower to medium elevations disappears. On the basis of three-year simulation results, the study basin is found predominantly a snow-fed as annual snowmelt runoff contribution to the river flow may ranges 65–75 %. About 66 % of the total runoff (46 % snowmelt and 20 % rainfall) is generated during four main summer months (i.e., May–August).

REFERENCES

1. PARC & ICIMOD. *Inventory of glaciers, glacial lakes and glacial lake outburst floods (GLOFs) in the mountains of Himalayan Region*. International Centre for Mountain Development (ICIMOD) and Pakistan Agricultural Research Council (PARC), Islamabad **(**2005).
2. Tarar, R.N. Water resources investigation in Pakistan with the help of Landsat imagery — snow surveys 1975-1978. Hydrological Aspects of Alpine and High Mountain Areas, *Proceedings of the Exeter Symposium.* IAHS Pub. No. 138 (1982).
3. Hewitt, K. Snow and ice hydrology in remote, high mountain regions: the Himalayan sources of the river Indus. *Snow and Ice Hydrology Project, Working Paper. No. 1*, Wilfred Laurier University, Waterloo, Ontario, Canada (1985).
4. Liu, X. & B. Chen. Climate warming in the Tibetan Plateau during recent decades. *International Journal of Climatology* 20**:** 1729-1742 (2000).
5. Ahmad, B. *Development of a distributed hydrological model coupled with satellite data for snowy basins.* PhD thesis, University of Tokyo, Japan (2005).
6. Rango, A., V.V. Salomonson & J.L. Foster Seasonal stream flow estimation in the Himalayan region employing meteorological satellites snowcover observations. *Water Resources Research* 13(1): 109-112 (1977).
7. Ehrer, C., K. Seidel & J. Martinec. *Advanced analysis of snow cover based on satellite remote sensing for the assessment of water resources.* Proceedings of the IAHS Symposium: Remote Sensing and Geographic Information Systems for Design and Operation of Water Resources Systems, Rabat, Morocco, *IAHS Pub*. 242: 93–101 (1997).
8. Martinec, J. Snowmelt-runoff model for streamflow forecasts. *Nordic Hydrology* 6: 145 – 154 (1975).
9. Schaper, J. & K. Seide. *Modeling daily runoff from snow and glacier melt using remote sensing data.* Proceedings of EARSeL-SIG-Workshop Land Ice and Snow, Dresden/FRG (2000)
10. Hong, M. & C. Guodong. A test of Snowmelt Runoff Model (SRM) for the Gongnaisi River basin in the western Tianshan Mountains, China *Chinese Science Bulletin* 48 (20): 2253-2259 (2003).
11. WMO. *Inter-comparison of models of snowmelt runoff. Operational Hydrology Report 23,* World Meteorological Organization (WMO), Geneva, Switzerland. WMO -No. 646 (1986).
12. WMO. *Simulated real-time inter-comparison of hydrological models. Operational Hydrol.* Report 38, *WMO*, Geneva, Switzerland (1992).
13. Seidel K., J. Martinec & M.F. Baumgartner. Modeling runoff and impact of climate change in large Himalayan Basins. *Integrated Water Resources for Sustainable Development* 2: 1020-1028 (2000).
14. Emre, T., A. Zuhal, S. Arda, Ş Aynur & Ş. Ünal. Using MODIS snow cover maps in modeling snowmelt runoff process in the eastern part of Turkey. *Remote Sensing of Environment* 97(2): 216-230 (2005).
15. Georgievsky, M.V. Application of the Snowmelt Runoff model in the Kuban river basin using MODIS satellite images. *Environ. Res. Lett. 4*. doi:10.1088/1748-9326/4/4/045017 (2009).
16. Hall, D.K., G.A. Riggs, & V.V. Salomonson. Development of methods for mapping global snow cover using moderate resolution imaging spectroradiometer data. *Remote Sensing of Environment* 54: 127-140 (1995).
17. Klein, A.G., D.K. Hall & G.A Riggs. Improving snow cover mapping in forests through the use of a canopy reflectance model. *Hydrological Processes* 12: 1723-1744 (1998).
18. Hall D.K., R.A. Riggs & V.V. Salomonson. Algorithm theoretical basis Document (ATBD) for MODIS snow & sea ice-mapping algorithms. http://modis.gsfc.nasa.gov/data/atbd/atbd_mod10.pdf. (2001).

19. Hall, D.K., G.A. Riggs, V.V. Salomonson, E.D. Nicolo & J.B. Klaus. MODIS snow-cover products, *Remote Sensing of Environment* 83: 181-194. doi:modis-snow-ice.gsfc.nasa.gov/ap_ snowcover02.pdf (2002).
20. Hall, D.K. & G.A. Riggs. Accuracy assessment of the MODIS snow products. *Hydrological Processes* 21: 1534 – 1547 (2007).
21. Riggs, G.A., D.K. Hall & V.V. Salomonson. MODIS snow products user guide to collection 5. doi:modis-snow-ice.gsfc.nasa.gov/sug_c5.pdf (2007).
22. Ackerman, S. A., KI.Strabala, P.W.P. Menzel, R.A. Frey, C.C. Moeller, & L.E. Gumley. Discriminating clear sky from clouds with MODIS. *Journal of Geophysical Research* 103: 32141– 32157 (1998).
23. Platnick S, M.D. King, S.A. Ackerman, W.P. Menzel, B.A. Baum, J.C. Ri´edi, R.A. Frei. The MODIS cloud products: algorithms and examples from Terra. *IEEE Transactions on Geoscience and Remote Sensing* 4: 459–473 (2003).
24. Key, J. R., J.B. Collins, C. Fowler, & R.S. Stone. High-latitude surface temperature estimates from thermal satellite data. *Remote Sensing of Environment* 61: 302– 309 (1997).
25. Salomonson, V.V. & I. Apppel. Estimating fractional snowcover from MODIS using the normalized difference snow index. *Remote Sensing of Environment* 89: 351-360 (2004).
26. Martinec, J. Snowmelt runoff model for stream flow forecasts. *Nordic Hydrology* 6: 145–154 (1975).
27. Martinec, J., A. Rango & R. Roberts. Snowmelt Runoff Model (SRM) User's Manual, Updated Edition for Windows, WinSRM Version 1.11 (2007).
28. Martinec, J. The degree-day factor for snowmelt runoff forecasting. IUGG General Assembly of Helsinki, IAHS Commission of Surface Waters, IAHS Publication No. 51, 468-477 (1960).
29. US Army Corps of Engineers. *Snow Hydrology, North Pacific Division.* Corps of Engineers, US Army, Portland, Oregon (1956).
30. Wilson, W. T. An outline of the thermodynamics of snow-melt. Trans. *Am. Geophys. Union,* Part 1, 182-195 (1941).
31. Ahmad, S. & M.F. Joya. *Northern Areas Strategy for Sustainable Development – Background Paper: Water.* IUCN Pakistan, Northern Areas Progamme, Gilgit, Pakistan (2003).
32. Singh, P., S. K. Jain, and N. Kumar, Estimation of snow and glacier-melt contribution to the Chenab River, Western Himalaya. *Mountain Research and Development* 17: 49-56. doi:links.jstor.org/sici?sici=0276-4741%28199702%2917%3A1%3C49%3AEOSAGC%3E2.0.CO%3B2-9 (1997).
33. K.M. Siddiqui, S. Ahmad, A.R. Khan, A. Bari, M.M. Sheikh & A.H. Khan. *Global change impact assessment for the Himalayan mountain regions of Pakistan, country case studies of Siran and Hunza Valleys.* Report-2002, APN Project # 2002-03 (2003).